J|A|C|S
ARTICLES

Published on Web 11/19/2009

Thermodynamic Analysis of mRNA Cap Binding by the Human Initiation Factor eIF4E via Free Energy Perturbations

Cristiano R. W. Guimarães,[†] David J. Kopecky,[‡] Jeff Mihalic,[‡] Shanling Shen,[§] Shawn Jeffries,[§] Stephen T. Thibault,[†] Xiaoqi Chen,[‡] Nigel Walker,[†] and Mario Cardozo*[,†]

Departments of Molecular Structure, Medicinal Chemistry, and Oncology, Amgen, Inc., 1120 Veterans Boulevard, South San Francisco, California 94080

Received July 30, 2009; E-mail: mcardozo@amgen.com

Abstract: Eukaryotic mRNAs are appended at the 5′ end, with the 7-methylguanosine cap linked by a 5′−5′-triphosphate bridge to the first transcribed nucleoside (m7GpppX). Initiation of cap-dependent translation of mRNA requires direct interaction between the cap structure and the eukaryotic translation initiation factor eIF4E. Biophysical studies of the association between eIF4E and various cap analogs have demonstrated that m^7GTP binds to the protein ca. −5.0 kcal/mol more favorably than unmethylated GTP. In this work, a thermodynamic analysis of the binding process between eIF4E and several cap analogs has been conducted using Monte Carlo (MC) simulations in conjunction with free energy perturbation (FEP) calculations. To address the role of the 7-methyl group in the eIF4E/m7GpppX cap interaction, binding free energies have been computed for m^7GTP, GTP, protonated GTP at N(7), the 7-methyldeazaguanosine 5′-triphosphate (m^7DTP), and 7-deazaguanosine 5′-triphosphate (DTP) cap analogs. The MC/FEP simulations for the GTP→m^7DTP transformation demonstrate that half of the binding free energy gain of m^7GTP with respect to GTP can be attributed to favorable van der Waals interactions with Trp166 and reduced desolvation penalty due to the N(7) methyl group. The methyl group both eliminates the desolvation penalty of the N(7) atom upon binding and creates a larger cavity within the solvent that further facilitates the desolvation step. Analysis of the pair m^7GTP−m^7DTP suggests that the remaining gain in affinity is related to the positive charge created on the guanine moiety due to the N(7) methylation. The charge provides favorable cation−π interactions with Trp56 and Trp102 and decreases the negative molecular charge, which helps the transfer from the solvent, a more polar environment, to the protein.

Introduction

Eukaryotic mRNAs are appended at the 5′ end, with the 7-methylguanosine cap linked by a 5′−5′-triphosphate bridge to the first transcribed nucleoside (m7GpppX).[1] The cap structure plays a pivotal role in several stages of gene expression, such as promoting mRNA splicing, facilitating mRNA export to the cytoplasm, and protecting mRNA against nucleolytic degradation.[2] The cap structure is also important for mRNA stabilization and ribosome recruitment for translation.[3] In cap-dependent translation, a direct interaction is required between the cap structure and the eukaryotic initiation factor 4E (eIF4E) for efficient translation initiation.[4,5] eIF4E, which is phylogenetically highly conserved, is the smallest subunit (25 kDa) of the eIF4F heterotrimeric complex. In addition to eIF4E, this complex contains the scaffold protein, eIF4G, and an RNA helicase, eIF4A.[6] Upon cap binding, eIF4F and another initiation factor, eIF4B, unwind secondary structure within the 5′ untranslated region of mRNA and enable recruitment of the ribosome to the translation start codon.[5]

eIF4E is the least abundant initiation factor; its recruitment to mRNA is suspected to be the rate-limiting step in new protein synthesis.[7] The accessibility of eIF4E in mammals is regulated by interactions with the small eIF4E-binding proteins, 4E-BP1, 4E-BP2, and 4E-BP3, which prevent productive interactions between eIF4E and eIF4G.[8,9] Phosphorylation of 4E-BPs by active mTOR, the mammalian target of rapamycin, leads to a significant loss of their binding ability to eIF4E, which facilitates association of eIF4E and eIF4G, and new protein synthesis.[10]

Upregulation of eIF4E cap dependent protein translation is commonly observed in multiple human tumor types. Activation of eIF4E lies downstream of growth factor signaling through

[†] Department of Molecular Structure.
[‡] Department of Medicinal Chemistry.
[§] Department of Oncology.

(1) Niedzwiecka, A.; Marcotrigiano, J.; Stepinski, J.; Jankowska-Anyszka, M.; Wyslouch-Cieszynska, A.; Dadlez, M.; Gingras, A.-C.; Mak, P.; Darzynkiewicz, E.; Sonenberg, N.; Burley, S. K.; Stolarski, R. *J. Mol. Biol.* **2002**, *319*, 615–635.
(2) Furuichi, Y.; Shatkin, A. J. *Adv. Virus Res.* **2000**, *55*, 135–184.
(3) Miura, K. *Advan. Biophys.* **1981**, *14*, 205–238.
(4) Pain, V. M. *Eur. J. Biochem.* **1996**, *236*, 747–771.
(5) Gingras, A.-C.; Raught, B.; Sonenberg, N. *Annu. Rev. Biochem.* **1999**, *68*, 913–963.
(6) Niedzwiecka, A.; Darzynkiewicz, E.; Stolarski, R. *Biochemistry* **2004**, *43*, 13305–13317.
(7) Raught, B.; Gingras, A.-C. *Int. J. Biochem. Cell Biol.* **1999**, *31*, 43–57.
(8) Haghighat, A.; Mader, S.; Pause, A.; Sonenberg, N. *Eur. Mol. Biol. Org. J.* **1995**, *14*, 5701–5709.
(9) Mader, S.; Lee, H.; Pause, A.; Sonenberg, N. *Mol. Cell. Biol.* **1995**, *15*, 4990–4997.
(10) Reiling, J. H.; Sabatini, D. M. *Oncogene* **2006**, *25*, 6373–6383.

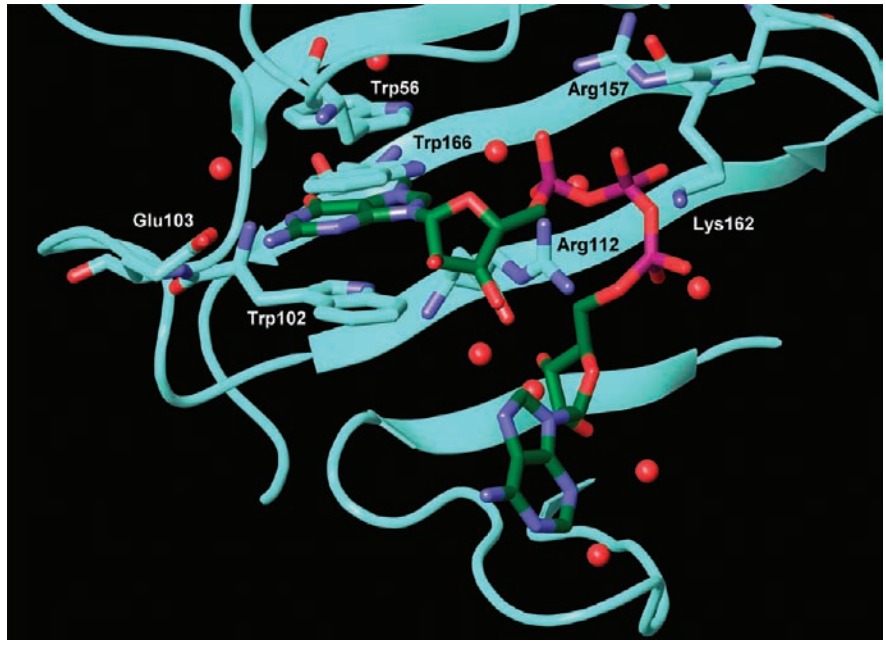

Figure 1. Interactions between m^{7}GpppA and human eIF4E observed in the crystal structure (Brookhaven Protein Data Bank code 1WKW).

the PI3K−Akt−mTor pathway; signaling via this network is frequently upregulated during human tumorigenesis.[11] Overexpression of eIF4E causes accelerated cell division, malignant transformation, and inhibition of apoptosis.[5] eIF4E overexpression occurs up to 30-fold in many cancers, including head and neck, breast, and lung cancers.[6] Levels of eIF4E are also elevated in some colon carcinomas in comparison to normal colon cells.[12,13] In certain types of cancer, the relationship between 4E-BP1 and eIF4E might be a predictor of metastasis.[14] Both eIF4E and 4E-BP1 are frequently overexpressed in colon carcinoma, but the 4E-BP1 levels are the most elevated in patients that have little or no metastatic disease.[14] This overexpression of eIF4E observed in several tumor types suggests that the development of an inhibitor of eIF4E could be a suitable anticancer therapeutic approach, since it has the potential to interfere in cap-dependent translation of mRNA and in turn decrease cell proliferation.

X-ray crystal structures of human eIF4E and the cap analogs m^{7}GTP and m^{7}GpppA as well as the ternary complex of eIF4E, m^{7}GpppA, and a 4E-BP1 fragment have been determined.[15,16] The 4E-BP1 fragment does not significantly affect the overall tertiary structure and cap-binding scaffold of eIF4E.[16] eIF4E forms a temple-bell-shaped surface of eight antiparallel β-structures, three α-helices, and ten loop structures, where the N-terminal region corresponds to the handle of the bell.[15] The m^{7}G moiety of m^{7}GpppA displays multiple interactions with eIF4E; two hydrogen bonds with the Glu103 side chain and one with the backbone NH of Trp102, cation$-\pi$ interactions with Trp102 and Trp56, and van der Waals interactions between the N(7)-methyl group and Trp166 (Figure 1). The triphosphate moiety forms an extensive hydrogen-bonding network with Arg112, Arg157, Lys162, and water molecules. Finally, the adenosine moiety interacts with the flexible C-terminal loop region, unobserved for the complex with m^{7}GTP.

Biophysical studies at 20 °C of the association between murine eIF4E and various cap analogs have been reported.[1] There are clearly profound effects on the binding free energies obtained following modifications of the cap structure. One of the most striking differences is a 5000-fold drop in the association constant or a binding free energy ca. 5.0 kcal/mol less favorable for GTP as compared to m^{7}GTP. The only direct interaction involving the 7-methyl group is a nonspecific van der Waals contact with Trp166 (Figure 1), suggesting the eIF4E binding enhancement for m^{7}GTP might derive from favorable cation$-\pi$ interactions between the resultant positive charge at the m^{7}G moiety and the Trp102 and Trp56 residues. Another contribution for the lower eIF4E affinity of GTP is potentially associated with its greater desolvation penalty upon binding; GTP has an additional negative charge when compared to m^{7}GTP. Also, the N(7) atom of the former is available to form hydrogen-bond interactions with water molecules in the unbound state.

In this work, a thermodynamic analysis of the eIF4E binding process has been conducted using Monte Carlo (MC)[17] simulations in conjunction with free energy perturbation (FEP) calculations.[18−21] More specifically, the relative eIF4E binding free energy between m^{7}GTP and GTP was computed. To understand the role of the 7-methyl group in the greater affinity of m^{7}GTP, relative binding free energies were also computed

(11) Easton, J. B.; Houghton, P. J. *Oncogene* **2006**, *25*, 6436–6446.
(12) Rosenwald, I. B.; Chen, J. J.; Wang, S.; Savas, L.; London, I. M.; Pullman, J. *Oncogene* **1999**, *18*, 2507–2517.
(13) Berkel, H. J.; Turbat-Herrera, E. A.; Shi, R.; de Benedetti, A. *Cancer Epidemiol. Biomarkers Prev.* **2001**, *10*, 663–666.
(14) Martin, M. E.; Perez, M. I.; Redondo, C.; Alvarez, M. I.; Salinas, M.; Fando, J. L. *Int. J. Biochem. Cell Biol.* **2000**, *32*, 633–642.
(15) Tomoo, K.; Shen, X.; Okabe, K.; Nozoe, Y.; Fukuhara, S.; Morino, S.; Sasaki, M.; Taniguchi, T.; Miyagawa, H.; Kitamura, K.; Miura, K.-I.; Ishida, T. *J. Mol. Biol.* **2003**, *328*, 365–383.
(16) Tomoo, K.; Matsushitaa, Y.; Fujisakia, H.; Abiko, F.; Shena, X.; Taniguchib, T.; Miyagawac, H.; Kitamurac, K.; Miurad, K.-I.; Ishidaa, T. *BBA* **2005**, *1753*, 191–208.
(17) Allen, M. P.; Tildesley, D. J. *Computer Simulations of Liquids*; Clarendon Press: Oxford, U.K., 1987.
(18) Zwanzig, R. *J. Chem. Phys.* **1954**, *22*, 1420–1426.
(19) Jorgensen, W. L.; Ravimohan, C. *J. Chem. Phys.* **1985**, *83*, 3050–3056.
(20) Jorgensen, W. L. *Acc. Chem. Res.* **1989**, *22*, 184–189.
(21) Kollman, P. A. *Chem. Rev.* **1993**, *93*, 2395–2417.

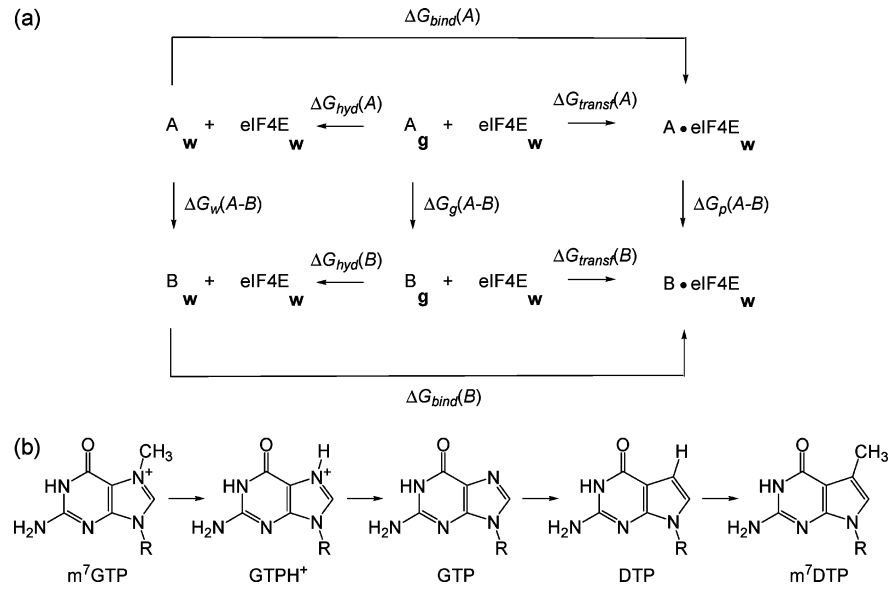

Figure 2. (a) Thermodynamic cycles used for the calculation of relative free energies. ΔG_{hyd}, ΔG_{transf}, and ΔG_{bind} are the absolute free energies of hydration, transfer from the gas phase to the solvated protein, and binding. ΔG_g, ΔG_w, and ΔG_p are the free energy changes for the transformation of ligand **A** into **B** in the gas phase, water, and protein. (b) Transformation sequence used in the FEP simulations.

for protonated GTP at N(7) ($GTPH^+$) and the 7-methyldeazaguanosine 5′-triphosphate (m^7DTP) and 7-deazaguanosine 5′-triphosphate (DTP) cap analogs. In addition, in order to verify the influence of hydration on the binding process, the relative free energies of hydration for the analogs were calculated. The experimental result for nucleotide analogs with a positive charge and neutral core validates our hypothesis of the various binding contributions. This in turn provides insight into ligand design aimed to develop an eIF4E inhibitor with potential application in anticancer therapy.

Computational Details

Free Energy Changes. Figure 2 illustrates the thermodynamic cycles used to calculate the free energy changes.[22] Since free energy is a thermodynamic state function, the cycle on the left side of Figure 2a gives the relative free energy of hydration (eq 1), where **A** and **B** are any two analogs, ΔG_{hyd} is the absolute free energy of hydration, and $\Delta G_w(\mathbf{A}\rightarrow\mathbf{B})$ and $\Delta G_g(\mathbf{A}\rightarrow\mathbf{B})$ are the free energies associated with the transformation of ligand **A** into **B** in water and in the gas phase, respectively.

$$\Delta\Delta G_{hyd} = \Delta G_{hyd}(\mathbf{B}) - \Delta G_{hyd}(\mathbf{A}) = \Delta G_w(\mathbf{A} \rightarrow \mathbf{B}) - \Delta G_g(\mathbf{A} \rightarrow \mathbf{B}) \quad (1)$$

The cycle on the right-hand side of Figure 2a gives the relative free energy of transfer from the gas phase to the solvated protein between **A** and **B**. In eq 2, ΔG_{transf} is the absolute free energy of transfer and $\Delta G_p(\mathbf{A}\rightarrow\mathbf{B})$ is the free energy associated with the transformation of **A** into **B** in the solvated eIF4E.

$$\Delta\Delta G_{transf} = \Delta G_{transf}(\mathbf{B}) - \Delta G_{transf}(\mathbf{A}) = \Delta G_p(\mathbf{A} \rightarrow \mathbf{B}) - \Delta G_g(\mathbf{A} \rightarrow \mathbf{B}) \quad (2)$$

Finally, relative binding free energies, $\Delta\Delta G_{bind}$, can be rewritten as the difference between $\Delta\Delta G_{transf}$ and $\Delta\Delta G_{hyd}$ as shown in eq 3, where ΔG_{bind} is the absolute binding free energy. In this manner, the binding process is separated into dehydration and transfer from the gas phase to the protein, thus facilitating the rationalization of the affinity order. The required $\Delta G(\mathbf{A}\rightarrow\mathbf{B})$ terms are computed by transforming **A** into **B** in the different environments through the FEP methodology using the sequence shown in Figure 2b.[19]

$$\Delta\Delta G_{bind} = \Delta G_{bind}(\mathbf{B}) - \Delta G_{bind}(\mathbf{A}) = \Delta G_p(\mathbf{A} \rightarrow \mathbf{B}) - \Delta G_w(\mathbf{A} \rightarrow \mathbf{B}) = \Delta\Delta G_{transf} - \Delta\Delta G_{hyd} \quad (3)$$

Protein−Ligand Complexes. The crystal structure for the 2.1 Å ternary complex between human eIF4E, m^7GpppA, and the 4E-BP1 peptide (only the Pro47-Pro66 sequence of human 4E-BP1 was determined) was employed (Brookhaven Protein Data Bank code 1WKW).[16] All cocrystallized water molecules as well as 4E-BP1 were removed from the complex. m^7GpppA was converted into m^7GTP by simple deletion of adenosine. The segment from N-terminal to Gln26 was not determined experimentally because of low electron density.[16] As this region is very far from the binding site, it was not considered in the model, which only contains residues 27 to 217 plus m^7GTP. A restrained conjugate-gradient energy minimization for the complex between eIF4E and m^7GTP was performed to alleviate bad contacts in the crystal structure. The energy minimization step was stopped when a backbone deviation of 0.3 Å with respect to the starting structure was reached. Degrees of freedom for the protein backbone atoms were not sampled in the MC simulations. Only the bond angles and dihedral angles for the side chains of residues with any atom within 10 Å from m^7GTP were varied. The ligands, however, are fully flexible in the MC simulations except as specified below. The pK_2 value of the m^7GTP γ-phosphate group is close to 7.[1] As the association between m^7GTP and eIF4E is practically the same for pH values ranging from 6.0 to 8.5,[1] the γ-phosphate group was considered here in its monoanionic state. Thus, partial atomic charges totaling −2 e for m^7GTP and $GTPH^+$ and −3 e for GTP, DTP, and m^7DTP were computed using the CM1A procedure.[23]

(22) Wong, C. F.; McCammon, J. A. *J. Am. Chem. Soc.* **1986**, *108*, 3830–3832.

(23) Storer, J. W.; Giesen, D. J.; Cramer, C. J.; Truhlar, D. G. *J. Comput-Aided Mol. Design* **1995**, *9*, 87–110.

The preparation of the enzymatic system was much facilitated by use of the Chop delegate program.[24] Charge neutrality for the protein was imposed by assigning normal protonation states at physiological pH to basic and acidic residues near the active site and making the adjustments for neutrality to the most distant residues. As for the protonation and tautomeric states for histidine residues, the defaults in the Chop software were employed. The entire system was solvated with a 22 Å radius water cap consisting of 852 molecules. A half-harmonic potential with a force constant of 1.5 kcal/mol·Å^2 was applied to water molecules at distances greater than 22 Å from the center of the system to discourage evaporation. As discussed previously,[25] the use of a spherical cap of water rather than periodic boundary conditions affects the calculated free energies of hydration in simple systems. Therefore, to cancel any potential errors, a 22 Å cap with 1474 water molecules was also used for the **A→B** unbound perturbations, yielding ΔG_w(**A→B**).

MC Simulations. The **A→B** transformations in all environments were performed using the single topology approach by melding the force field parameters for bond lengths, bond angles, torsions, and nonbonded interactions.[19] In order to keep the number of atoms constant, dummy (DM) atoms were introduced for hydrogens that exist in one state and have no counterpart in the other. Bond lengths for perturbations requiring an atom mutation or an annihilation or creation of a hydrogen were not sampled and were treated as geometrical parameters. Bonds containing a DM atom have an equilibrium value of 0.5 Å. Shrinking the bond length for DM atoms is a common practice to improve convergence in FEP simulations.[19,26−29] The bond angles involving dummy atoms have the same parameters as their counterparts in the other state. Associated unphysical contributions to the free-energy differences cancel in a thermodynamic cycle.[26,28] The MC/FEP calculations for the **A→B** transformations were executed at 25 °C using double-wide sampling.[19] Residue-based cutoffs of 10 Å were employed in all transformations except the one from GTPH$^+$ to GTP. As this transformation involves a charge mutation from −2 to −3 e, no cutoffs were applied. In this manner, since the water-phase and solvated eIF4E models have equal radii and the same dielectric constant outside the spherical system, the missing long-range electrostatic interactions between the solvent molecules not included in the finite models and the ligands with different molecular charges would cancel out when computing $\Delta\Delta G_{bind}$ for the GTPH$^+$→GTP transformation.

The initial and final states were coupled using 10 windows with values for the coupling parameter (λ) evenly distributed between 0 and 1 (0.05, 0.15, ..., 0.85, 0.95). Initial relaxation of the solvent was performed for 5×10^6 configurations, followed by 20×10^6 configurations of full equilibration and 30×10^6 configurations of data collection for each window in water or protein, whereas for the gas-phase simulations, 5×10^6 configurations of equilibration and 10×10^6 configurations of data collection were employed. The ΔG values obtained for each window are averages of six independent MC runs, giving a total of 3.3×10^9 configurations per ΔG_w(**A→B**) and ΔG_p(**A→B**) values and 0.9×10^9 configurations per ΔG_g(**A→B**) value. Since no cutoffs were used for the GTPH$^+$→GTP transformation, 5×10^6 configurations of full equilibration and 10×10^6 configurations of data collection were applied for each window in water or protein to reduce the computational cost for these simulations. This is possible because only the partial charges (the hydrogen atom connected to the N(7) atom has no Lennard-Jones parameters) are perturbed in this transformation, providing a very fast convergence for the free energy values obtained. The independent FEP simulations for each pair of ligands were all performed in the same direction, according to the convention shown in Figure 2b. The energy-minimized crystal structure for the complex between eIF4E and m^{7}GTP provided the initial configuration for the FEP simulations in all complex environments. The other five starting configurations per transformation were randomly selected from the equilibration phase of each respective first FEP run at a λ value of 0.05. A similar scheme was applied to the simulations in the gas phase and water.

MCPRO 2.0 was used to perform all MC calculations.[30] Established procedures including Metropolis and preferential sampling were employed, and statistical uncertainties were obtained from the batch means procedure with batch sizes of 1×10^6 configurations.[17] Attempted moves of the cap analogs in water occurred every 10 configurations, while, in the complex, attempted moves of the protein and cap analogs occurred every 10 and 80 configurations, respectively. The TIP4P model[31] was used for water, and the complexes were represented with the OPLS-AA force field,[32] with the exception of the CM1A atomic charges for the ligands.

Experimental Details

In Vitro IC_{50} Determination of eIF4E m^{7}GTP Binding. Human eIF4E protein (NP_001959) was produced as an N terminal FLAG-HIS fusion protein in BL21 bacterial cells and purified by m^{7}GTP−Sepharose affinity chromatography (GE Healthcare). Protein was eluted with 100 μM m^{7}GDP and dialyzed extensively into storage buffer. For binding analysis, eIF4E protein (50nM final) was biotinylated and bound to streptaviden-coated scintillation proximity assay beads (GE Healthcare) in the presence of ^{3}H-m^{7}GTP (1mCi/mL, Moravek Biochemicals) in binding buffer (20 mM HEPES, pH 7.4, 50 mM KCL, 1 mM DTT and 0.5 mM EDTA). To determine competitive inhibition of eIF4E binding, compounds were added in an 11-point, 3-fold dilution dose series, and loss of radioactive signal was monitored by scintillation counting. IC_{50} values were calculated by nonlinear regression curve fitting using GraphPad Prism analysis software (GraphPad Software).

Chemical Synthesis. Synthetic route and procedure for the preparation of compounds **1** and **2** are provided in the Supporting Information.

Results and Discussion

Long MC/FEP simulations were performed generating smooth free-energy curves for the **A→B** transformations in all environments (Figure 3). As noted above (eqs 1−3), the binding process may be decomposed into dehydration and transfer from the gas phase to the protein. The relative free energies, $\Delta\Delta G_{transf}$, $\Delta\Delta G_{hyd}$, and $\Delta\Delta G_{bind}$, between all cap analogs are reported in Table 1.

(24) Tirado-Rives, J. *Chop*; Yale University: New Haven, CT, 2002.
(25) Essex, J.; Jorgensen, W. L. *J. Comput. Chem.* **1995**, *16*, 9510–972.
(26) Boresch, S.; Karplus, M. *J. Phys. Chem. A* **1999**, *103*, 103–118.
(27) Pearlman, D. A.; Kollman, P. A. *J. Chem. Phys.* **1991**, *94*, 4532–4545.
(28) Price, D. J.; Jorgensen, W. L. *J. Comput-Aided Mol. Design* **2001**, *15*, 681–695.
(29) Guimarães, C. R. W.; Boger, D. L.; Jorgensen, W. L. *J. Am. Chem. Soc.* **2005**, *127*, 17377–17384.
(30) Jorgensen, W. L. *MCPRO, Version 2.0*; Yale University: New Haven, CT, 2005.
(31) Jorgensen, W. L.; Chandrasekhar, J.; Madura, J. D.; Impey, W.; Klein, M. L. *J. Chem. Phys.* **1983**, *79*, 926–935.
(32) Jorgensen, W. L.; Maxwell, D. S.; Tirado-Rives, J. *J. Am. Chem. Soc.* **1996**, *118*, 11225–11236.

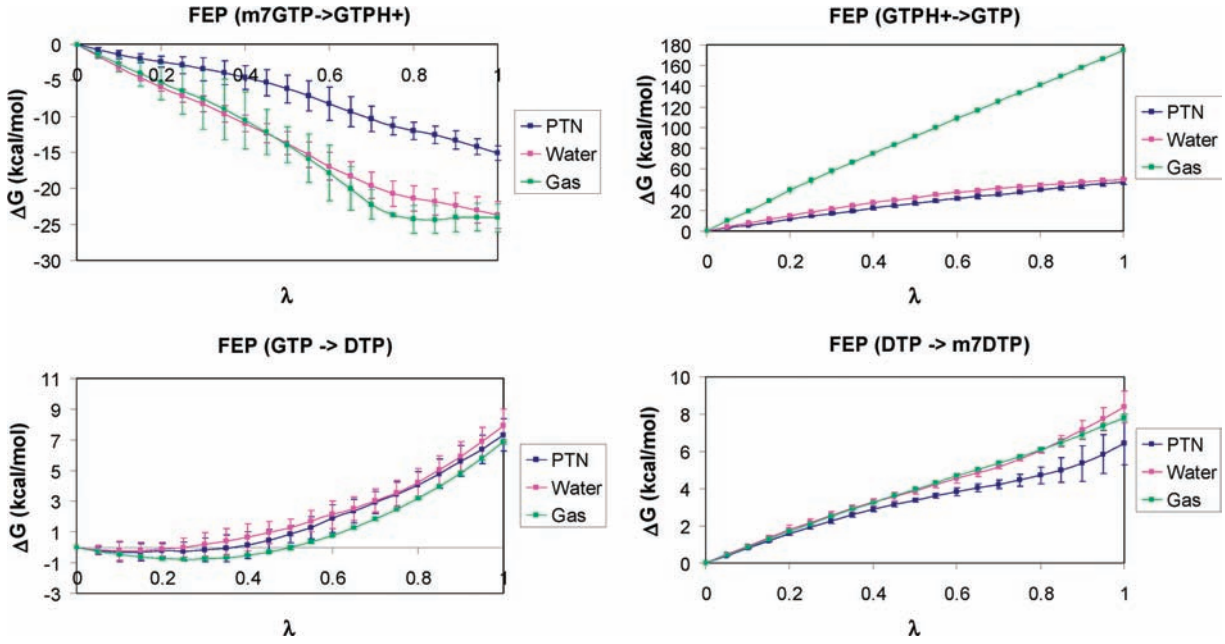

Figure 3. Free-energy curves obtained in the gas phase, water, and the protein for all transformations. Error bars representing two standard deviations from the six independent MC runs per window are also plotted. Error bars cannot be visualized for the $GTPH^+ \rightarrow GTP$ transformation due to the plot scale.

Table 1. Calculated Relative Free Energies of Transfer from the Gas Phase to eIF4E ($\Delta\Delta G_{transf}$), Hydration Free Energies ($\Delta\Delta G_{hyd}$), and Binding Free Energies ($\Delta\Delta G_{bind}$) between All Cap Analogs[a]

A → B[b]	m^7GTP	$GTPH^+$	GTP	DTP	m^7DTP
m^7GTP	0.0	9.0 ± 0.3	−117.9 ± 0.6	−117.5 ± 0.7	−118.9 ± 0.7
	0.0	0.4 ± 0.4	−124.3 ± 0.6	−123.2 ± 0.7	−122.6 ± 0.7
	0.0	**8.6 ± 0.3**	**6.4 ± 0.7**	**5.7 ± 0.8**	**3.7 ± 0.8**
$GTPH^+$		0.0	−126.9 ± 0.5	−126.5 ± 0.6	−127.9 ± 0.6
		0.0	−124.7 ± 0.5	−123.6 ± 0.6	−123.0 ± 0.6
		0.0	**−2.2 ± 0.6**	**−2.9 ± 0.7**	**−4.9 ± 0.7**
GTP			0.0	0.4 ± 0.4	−1.0 ± 0.4
			0.0	1.1 ± 0.4	1.7 ± 0.4
			0.0	**−0.7 ± 0.4**	**−2.7 ± 0.4**
DTP				0.0	−1.4 ± 0.2
				0.0	0.6 ± 0.2
				0.0	**−2.0 ± 0.2**
m^7DTP					0.0
					0.0
					0.0

[a] Values are in kcal/mol. $\Delta\Delta G_{transf}$, $\Delta\Delta G_{hyd}$, and $\Delta\Delta G_{bind}$, which are the first, second, and third values for each comparison in the table, were obtained according to eqs 1−3. $\Delta\Delta G_{bind}$ are highlighted in bold for clarification. The errors in $\Delta\Delta G$ were calculated by propagating the statistical uncertainties obtained from the batch means procedure with batch sizes of 1×10^6 configurations for the individual ΔG_i values of each window used to compute the ΔG_p, ΔG_w, and ΔG_g values. [b] For each **A→B** transformation and corresponding relative free-energy values, ligand **A** is in the table column and ligand **B** in the table row.

m^7GTP versus GTP. The transformation from m^7GTP to GTP was performed in two steps, with $GTPH^+$ being a hypothetical intermediate state between the two analogs (Figure 2). $GTPH^+$ was introduced to reduce the computational cost for the $m^7GTP \rightarrow GTP$ transformation, as it avoids the need to run long MC simulations with no cutoffs for nonbonded interactions. More specifically, since the $m^7GTP \rightarrow GTPH^+$ transformation involves the perturbation of bonded terms and Lennard-Jones parameters, the free energy values converge very slowly and demand long MC simulations. As the molecular charge is the same in both states, the computational cost can be reduced by employing residue-based cutoffs of 10 Å. In the $GTPH^+ \rightarrow GTP$ transformation, cutoffs cannot be used because a charge mutation from −2 to −3 e is required. However, shorter simulations can be performed as only the partial charges are mutated; the free energy values converge very fast in this type of transformation. In addition, $GTPH^+$ is a valuable molecule to understand the greater affinity of m^7GTP, as it has the same net charge and the ability to establish cation−π interactions with Trp56 and Trp102. The charge distributions for m^7GTP and $GTPH^+$ are very similar, with the positive charge resulting from methylation or protonation delocalized throughout the guanine ring.

The MC configurations for $GTPH^+$ in water show that the protonated N(7) atom forms hydrogen bonds with the solvent. In the gas phase, the protonated N(7) atom is hydrogen bonded to the γ-phosphate group. The $\Delta\Delta G_{hyd}$ value of only 0.4 kcal/mol for the $m^7GTP \rightarrow GTPH^+$ transformation (Table 1) indicates that the more favorable interactions with the solvent for the latter are offset by the loss of the intramolecular hydrogen bond upon solvation, resulting in similar hydration free energies for both analogs. When transferred from the gas phase to eIF4E, however, the loss of the intramolecular hydrogen bond with the γ-phosphate group is not counterbalanced, as the protonated N(7) atom does not form any hydrogen bonds with the protein (Figure 4); this reduces ΔG_{transf} for $GTPH^+$ by 9.0 kcal/mol with respect to m^7GTP. As a consequence, the eIF4E binding for the first is 8.6 kcal/mol less favorable. Thus, even though $GTPH^+$ is able to establish cation−π interactions with Trp56 and Trp102, burying the cationic hydrogen-bond donor greatly penalizes its eIF4E binding with respect to m^7GTP.

The MC simulations show that the N(7) atom of GTP is hydrogen bonded to the solvent in the water phase. No intramolecular hydrogen bonds between the N(7) atom and the hydroxyl of the γ-phosphate group were observed in the gas phase. In this manner, and differently from $GTPH^+$, GTP does not have a penalty associated with the loss of intramolecular hydrogen bonds upon solvation, thus facilitating its hydration process. In addition, as the electrostatic component of the solvation free energy is proportional to the square of the

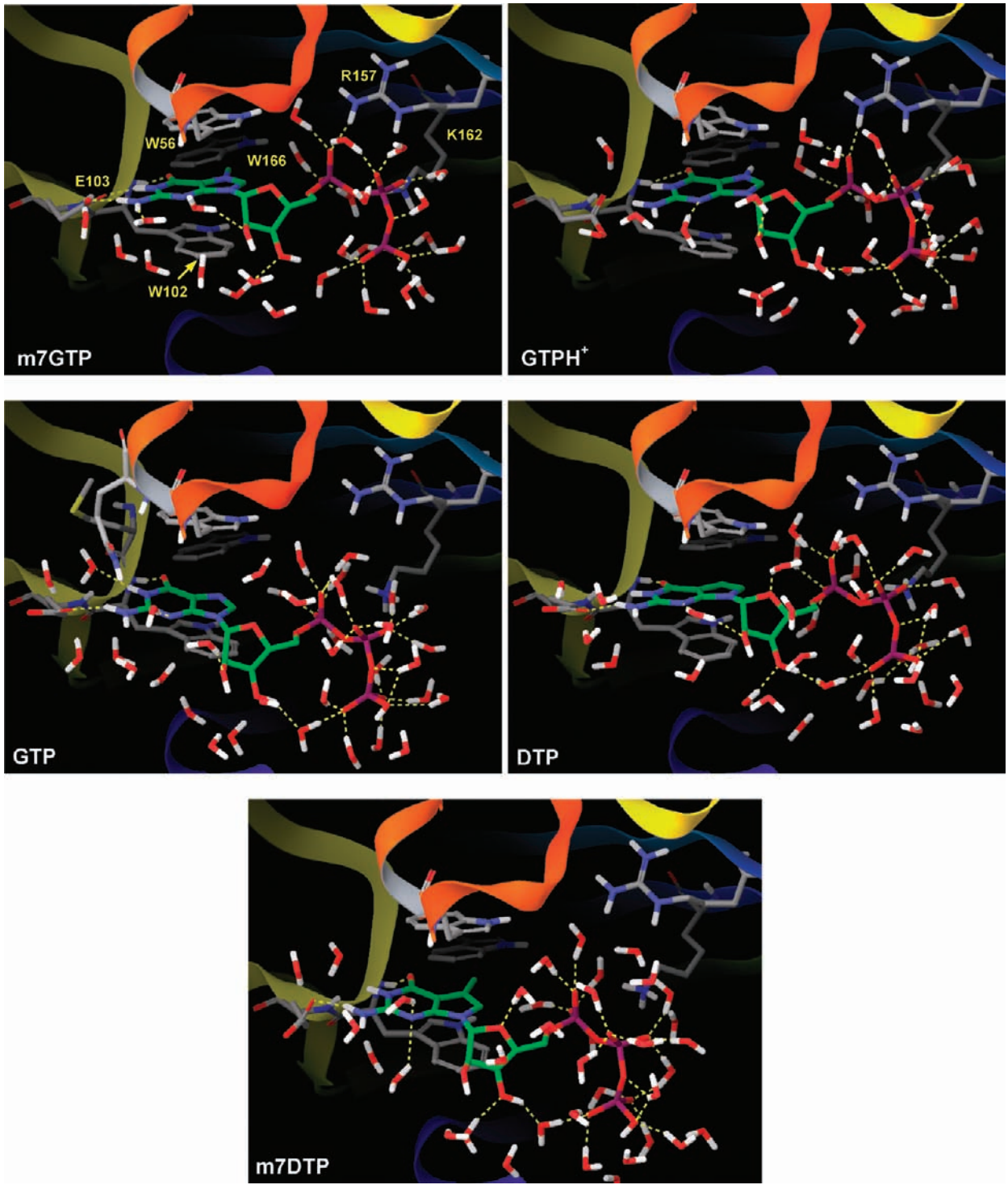

Figure 4. Monte Carlo snapshots illustrating the complexes between eIF4E and m^7GTP, $GTPH^+$, GTP, DTP, and m^7DTP.

molecular charge,[33] GTP, with a net charge of −3 e, should be significantly better hydrated than $GTPH^+$, which has a net charge of −2 e. The $\Delta\Delta G_{hyd}$ value in Table 1 indicates that the hydration of GTP is −124.7 kcal/mol more favorable than the one for $GTPH^+$. The correction of this value to account for the missing long-range electrostatic interactions between the solvent molecules not included in the finite models and the ligands with different molecular charges can be obtained via the Born equation.[33] It should be noted that exactly the same correction would be obtained for $\Delta\Delta G_{transf}$ as the solvated eIF4E has the same radius and dielectric constant outside the finite system; this correction then cancels out when computing $\Delta\Delta G_{bind}$ between $GTPH^+$ and GTP. Application of the Born equation to calculate the relative hydration between the 22 Å radius supermolecules with charges of −2 and −3 e, consisting of the solutes and all 1474 water molecules, results in a correction of −37.3 kcal/mol and provides a $\Delta\Delta G_{hyd}$ of −162.0 kcal/mol. The quality of this value can be attested by simple application of the Born equation to calculate the relative solvation free energy between ions with charges of −2 and −3

(33) Born, M. *Z. Phys.* **1920**, *1*, 45–48.

e and that have radii of ca. 5 Å. The agreement between the $\Delta\Delta G_{hyd}$ value calculated in this way and the one obtained from the FEP simulations and corrected as described above is very good.

The $\Delta\Delta G_{transf}$ value in Table 1 indicates that the transfer of GTP from the gas phase to the protein is −126.9 kcal/mol (−164.2 kcal/mol if corrected by the Born equation) more favorable than the one for $GTPH^+$. The eIF4E binding site is quite polar and exposed to the solvent. Thus, the additional negative charge of GTP provides a ΔG_{transf} value that is significantly more favorable than the one obtained for its protonated form. Also, as mentioned above, the transfer of $GTPH^+$ from the gas phase to the protein is greatly penalized due to the loss of intramolecular ionic hydrogen bonds in the gas phase and the burying of the cationic hydrogen-bond donor in a hydrophobic pocket of the protein. Hence, despite its significant desolvation penalty, GTP has greater affinity (−2.2 kcal/mol) for eIF4E than $GTPH^+$.

The combination of the results for the $m^7GTP \rightarrow GTPH^+$ and $GTPH^+ \rightarrow GTP$ transformations provides $\Delta\Delta G_{transf}$ of −117.9 kcal/mol, $\Delta\Delta G_{hyd}$ of −124.3 kcal/mol, and $\Delta\Delta G_{bind}$ of 6.4 kcal/mol between m^7GTP and GTP (Table 1). The calculated value is in very good agreement with the experimental value of 5.0 kcal/mol,[1] even without the application of a polarizable force field, believed to be important for the complete description of cation−π interactions. Contributions from polarization effects might not be as significant as for typical cation−π interactions, since the positive charge is highly delocalized throughout the guanine ring. Like before, the large negative values for $\Delta\Delta G_{transf}$ and $\Delta\Delta G_{hyd}$ are caused by the additional negative charge of GTP. In summary, the reduced affinity for GTP is derived from a large desolvation penalty that is not compensated for in the protein. The N(7) methylation (i) provides van der Waals interactions with Trp166, (ii) generates a positive charge that establishes cation−π interactions with Trp56 and Trp102, and (iii) facilitates the desolvation step because it reduces the molecular charge and eliminates the interactions between the N(7) atom of GTP and water molecules in the unbound state.

Role of the Methyl Group in the eIF4E Binding. Even though the binding process was separated into dehydration and transfer from the gas phase to the protein to facilitate the rationalization of the affinity order, it is still very difficult to pinpoint the specific contributions of the methyl group to $\Delta\Delta G_{hyd}$, $\Delta\Delta G_{transf}$, and $\Delta\Delta G_{bind}$ between m^7GTP and GTP. The net charge difference between these analogs further complicates the analysis due to the long-range electrostatic contributions to solvation and transfer from the gas phase to eIF4E. Therefore, in order to investigate what makes GTP have a poorer affinity for eIF4E, the GTP→DTP and DTP→m^7DTP transformations were also performed. DTP is an interesting model system to understand the penalty associated with the desolvation of the GTP N(7) atom upon binding, while m^7DTP, which cannot interact with Trp56 and Trp102 through cation−π interactions, addresses the binding contributions derived from the van der Waals interactions between the methyl group and Trp166.

Table 1 shows that the transfer from the gas phase to eIF4E is only 0.4 kcal/mol less favorable for DTP than GTP, suggesting that both analogs interact with similar strength with the protein through salt bridges, hydrogen bonds, and $\pi-\pi$ stacking interactions (Figure 4). However, the interactions between the solvent and the N(7) atom in the unbound state provide a more favorable hydration free energy for GTP. Thus, the greater desolvation penalty reduces the binding free energy of GTP by 1.1 kcal/mol. The final $\Delta\Delta G_{bind}$ value for the GTP→DTP transformation is then −0.7 kcal/mol.

For the DTP→m^7DTP transformation, the addition of a methyl group decreases the solvation of m^7DTP by 0.6 kcal/mol, which is likely related to the more unfavorable free energy required to form a larger cavity within the solvent; this component of the solvation free energy comprises the entropic penalty associated with the reorganization of the solvent molecules around the solute and the work done against the solvent pressure in creating the cavity. The transfer of m^7DTP from the gas phase to eIF4E is more favorable than that for DTP by −1.4 kcal/mol, indicating that the van der Waals interactions with Trp166 are indeed beneficial (Figure 4). Thus, the $\Delta\Delta G_{bind}$ value of −2.0 kcal/mol for the DTP→m^7DTP transformation consists of both more favorable desolvation and interactions with the protein due to the additional methyl group.

The combination of the results for the GTP→DTP and DTP→m^7DTP transformations provide $\Delta\Delta G_{hyd}$, $\Delta\Delta G_{transf}$, and $\Delta\Delta G_{bind}$ between GTP and m^7DTP (Table 1). With less solvation and more favorable transfer from the gas phase to eIF4E of 1.7 and −1.0 kcal/mol, respectively, m^7DTP binds more favorably than GTP by −2.7 kcal/mol. This corresponds to almost 55% of the experimental binding free energy gain of m^7GTP with respect to GTP (−5.0 kcal/mol) or 42% of the calculated value (−6.4 kcal/mol). In summary, the comparison of GTP with the deazaguanosine analogs indicates that a considerable portion of the relative binding free energy between m^7GTP and GTP can be attributed to favorable van der Waals interactions with Trp166 and reduced desolvation penalty due to the methyl group; the methyl group not only eliminates the penalty associated with the desolvation of the N(7) atom upon binding but also creates a larger cavity within the solvent that further facilitates the desolvation step. Analysis of the pair m^7GTP-m^7DTP suggests that the remaining boost in affinity is related to the positive charge created on the guanine moiety due to the N(7) methylation. It provides favorable cation−π interactions with Trp56 and Trp102 and decreases the negative molecular charge, which helps the transfer from the solvent, a more polar environment, to the protein.

Experimental Validation for the Cation−π Contribution. A medicinal chemistry program aimed at identifying a small molecule inhibitor of eIF4E has been conducted. The lead optimization process started from the cap analog m^7GTP. The initial goal of this effort was to obtain a tool compound showing eIF4E inhibitory activity in a relevant cellular assay. To this end, an inhibitor with high in vitro potency and suitable physicochemical properties for cellular permeability was required. During the course of the lead optimization effort, a large number of compounds were synthesized and the corresponding SAR results will be reported independently. Efforts focused upon reducing the total net charge of the molecule in order to improve cellular permeability while maintaining in vitro potency comparable to that of m^7GTP. Indeed, a suitable inhibitor design approach was to remove the positive charge from the nucleotide core. However, as mentioned previously, there is a 5000-fold loss in the binding affinity from m^7GTP to GTP ($\Delta\Delta G_{bind} \sim +5$ kcal/mol).[1] Nevertheless, our FEP studies of the $m^7GTP \rightarrow m^7DTP$ transformation suggested that the contribution of the cation−π interaction is worth about half of the total binding free energy loss from m^7GTP to GTP (Table 1). This result encouraged the synthesis of analogs with a neutral core which maintains other key groups important for binding. Here we illustrate the accuracy of our free energy estimations with two

Table 2. Molecular Structures and the Corresponding Experimental IC_{50} Values and Binding Free Energies for the eIF4E Inhibitors

Compound	Structure	IC_{50} (μM)	ΔG_{bind}[a] (kcal/mol)
1	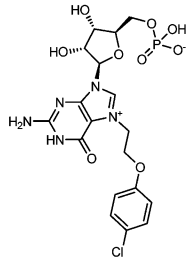	0.058	−9.87
2	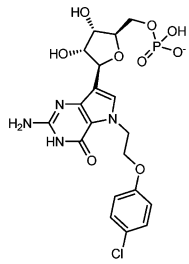	6.58	−7.05

[a] Calculated from $\Delta G_{bind} = RT \ln IC_{50}$ at 298 K.

examples of analogs where the main structural modification is the removal of the positive charge from the nucleotide core. Compounds **1** and **2** (Table 2) have the same substituents at the 7- and 9-positions of the nucleotide core. However, in **2** the core is neutral as a result of replacing the 9-position nitrogen atom in **1** with a carbon atom. On the basis of the fact that all of the substituents in **1** and **2** are identical, this pair of compounds provides an ideal case to study the importance of the cation−π interaction. The estimated ΔG_{bind} for compounds **1** and **2**, based on the measured IC_{50} values, are −9.9 and −7.1 kcal/mol, respectively. Thus, the loss in binding affinity for **2** of 2.8 kcal/mol is in good agreement with the calculated 3.7(±0.8) kcal/mol value for the m^7GTP→m^7DTP transformation (Table 1) and can be mainly attributed to the lack of cation−π interaction. GTP pays additional penalties upon binding, since its nitrogen lone pair is buried toward the protein surface, resulting in a large desolvation penalty without a compensating intermolecular interaction and reduced vdW interactions with the protein by not having the 7-position substituted with a methyl group. From the calculated binding free energy difference between m^7DTP and GTP (Table 1), these two effects combined account for about 2.7 kcal/mol of the total loss of binding from m^7GTP to GTP.

Conclusions

Striking aspects of the association between eIF4E and the cap analogs m^7GTP, GTP, protonated GTP at N(7) ($GTPH^+$), 7-deazaguanosine 5′-triphosphate (DTP), and 7-methyldeazaguanosine 5′-triphosphate (m^7DTP) have been addressed through the present free energy perturbation (FEP) simulations using Monte Carlo (MC) as the sampling technique. The MC/FEP simulations provided informative free energy results and computed structures. The rationalization of the affinity order obtained (m^7GTP > m^7DTP > DTP > GTP > $GTPH^+$) was greatly facilitated by the separation of the relative binding free energies into dehydration and transfer from the gas phase to the protein. The hypothetical analog $GTPH^+$ binds the least favorably to eIF4E because of the loss of the intramolecular hydrogen bond between the cationic hydrogen-bond donor and the γ-phosphate group that greatly penalizes the transfer from the gas phase to eIF4E. GTP has the second weakest affinity mainly because of loss of interactions between the solvent and the N(7) atom in the unbound state that are not compensated for in the protein. Simple transformation of GTP into DTP provides a gain in binding free energy of −0.7 kcal/mol, while methylation of the latter generating m^7DTP gives another −2.0 kcal/mol; the methyl group provides both favorable van der Waals interactions with Trp166 and reduced desolvation penalty due to larger cavity within the solvent that facilitates the desolvation step of m^7DTP. The more favorable m^7DTP-eIF4E binding of −2.7 kcal/mol with respect to GTP corresponds to almost 55% of the experimental relative binding free energy gain of m^7GTP with respect to GTP (−5.0 kcal/mol) or 42% of the calculated value (−6.4 kcal/mol). This suggests that almost half of the relative binding free energy between m^7GTP and GTP can be attributed to both favorable van der Waals interactions with Trp166 and reduced desolvation penalty due to the methyl group. The greater affinity of m^7GTP for eIF4E when compared to m^7DTP is due to the positive charge created on the guanine moiety because of the N(7) methylation. It provides favorable cation−π interactions with Trp56 and Trp102 and decreases the negative molecular charge, which likely reduces the desolvation penalty upon binding. Finally, the FEP simulations indicate that the cation−π interactions with Trp56 and Trp102 are important, but not as critical for eIF4E binding. When compared to m^7GTP, the affinity drop of GTP is 5000-fold while that for m^7DTP is only 50-fold. In other words, this work suggests that, when designing eIF4E inhibitors, neutral guanine analogs containing appropriate features can safely replace the positively charged 7-methylguanine core without significant losses in affinity. This hypothesis is in full agreement with the inhibitory potency observed for compound **2** and it provides a valid rationale for designing neutral eIF4E inhibitors with physicochemical properties suitable for cellular activity.

Acknowledgment. Gratitude is expressed to John Eksterowicz for helpful discussions.

Supporting Information Available: Synthetic route and procedure for the preparation of compounds **1** and **2**. This material is available free of charge via the Internet at http://pubs.acs.org.

JA9064359